Reply To Reviewer 1

We want to thank the reviewer for accepting our manuscript

Reply To Reviewer 2

We would like to thank Dr. Lambe for his insightful comments. Below we give point-by-point responses to the comments.

1. L93 – If the OFR254 mode is being used, I don't understand how the calculated OHexp value is now higher in the high-NO_x condition relative to the low-NO_x condition (in the absence of other changes): N2O creates an additional O(1D) sink, and NO2 creates additional OH reactivity. In the discussions paper, the OHexp values were 2.6e11 (low-NO_x) and 1.72e11 (high-NO_x); now, they are 1.82e12 (low-NO_x) and 2.45e12 (high-NO_x). In principle, it is possible to increase the OHexp in OFR185-iN2O due to N2O + hv185 -> O(1D) + N2, but I am not sure how that is possible with OFR254-iN2O. Unless I'm missing something, this doesn't seem right to me. I suggest double checking the model calculations and/or emailing me the KinSim mechanism (if Prof. Ng feels this is appropriate, given that the review is not anonymous) and we can try to straighten this out together.

Response: We double checked the model calculations. Indeed, the OH exposures that were estimated with KimSim were 1.82×10^{12} (low-NO_x) and 2.45×10^{12} (high-NO_x) molec cm^{-3} s. We acknowledge that the addition of N_2O would decrease the OH production in the OFR without changing the setting of the UV254 lamps. In order to keep the OH exposure close enough between two NO_x cases, we intentionally applied higher settings for the OH lamp in the high-NO_x case compared to the low-NO_x cases. The average photon fluxes were 1.08×10^{15} and 2.74×10^{15} photons cm^{-2} s^{-1} for the low- and high-NO_x cases, respectively. We added a sentence in section 2.1 to avoid any misunderstanding in the future. The reason for "*the OHexp values were 2.6*$\times10^{11}$ *(low-*NO_x*) and 1.72*$\times10^{11}$ *(high-*NO_x*); now, they are 1.82e12 (low-*NO_x*) and 2.45e12 (high-*NO_x*).*" can be due to the differences in the model settings between the simplified OFR model and the KinSim model.

Changes:

Section 2.1

[…] For the two NO_x cases, the voltage of the 254-nm lamps was adjusted to ensure similar OH exposure. […]

2. In regards to the authors' reply to my Comment #1, I will note that the model infrastructure outlined in Section 2.3 of Tikkanen et al. (2020) already exists, and the Kuopio group has the expertise to apply it here. It seems that the authors agree with the essence of my suggestion, but are mostly concerned about implementing it here because of the potential scope of the additional analysis that would be required. I will attempt to try to restrict the scope of what I am asking for in an attempt to make it more tractable, while also providing what I feel will be significant value added to the revised manuscript.

a. Because Tikkanen et al. (2020) already derived volatility distributions from evapograms of alpha-pinene SOA generated under low-NO_x conditions, it would be satisfactory to restrict the analysis to volatility distributions obtained from evapograms of the alpha-pinene SOA generated under high-NOx conditions here and compare to volatility distributions obtained from the corresponding FIGAERO-CIMS thermograms of high-NO_x alpha-pinene SOA

Response: We understood the strong wish from Dr. Lambe to compare the volatility distributions (VDs) between evapograms and FIGERO-CIMS thermograms in the same way as Tikkanen et al. (2020). As our manuscript and more detailed discussion below shows, our data and results point out that the aqueous-phase chemistry plays a significant role in this study. Unfortunately, the inverse model in Tikkanen et al., does not include aqueous-phase chemical processes, and as we show below, is not a suitable model for our system. Considering this, and the significant human resources needed to use the optimization algorithm correctly, we suggest an alternative approach.

To provide a comparison of the FIGAERO-CIMS data with the observed isothermal evaporation, we performed forward modelling for particle evaporation at high RH but without including any aqueous-phase chemistry. This can be done by using the VDs from the FIGAERO-CIMS thermograms collected at the fresh and high-RH stage as inputs for the same liquid-like evaporation model (LLEVAP) that was used in Tikkanen et al. (2020). With this setup, particle volatility is presumed as the only driver for particle size change in the simulation. The purpose is to see whether the use of FIGAERO-CIMS-derived VD can reproduce the observed isothermal evaporation at high RH. This approach is the same as that outlined in the last two paragraphs in Section 3.2 and shown in Figure 4 in Tikkanen et al. (2020).

The results of the model simulations are shown in Figure R1 a and b for the high- and low-NO_x cases at high RH, respectively. We found that the model simulations underestimated the particle evaporation rate (solid blue line in Fig R1a and b).

In Tikkanen et al. (2020), using the T_{50} values to characterize the volatility of each factor also led to an underestimation of the extent of evaporation (solid blue line in Figure R1c). But by allowing the desorption temperature of a PMF factor to vary in the range of the 25th and 75th percentile (Section 3.3 and Figure 5 in Tikkanen et al. (2020)), they were able to reproduce the observed evaporation of α-pinene SOA particles. Their result with the optimized VD is shown as the solid green line below in Fig. R1 c (see also Tikkanen et al. (2020) Figure. 5a). Similar agreement could not be achieved for our data (range given by shaded area in Figure R1a and b). The VD derived from the FIGAERO measurements in the present study is too far in the LVOC or ELVOC range, while 40% of the VD from Tikkanen et al. (2020) can be found in the SVOC range. The uncertainty range estimated from the 25th and 75th percentiles does not increase the volatility enough to match the evaporation observed in the thermograms. Therefore, the discrepancy between the simulated and observed evaporation curves in our study very likely suggests the significant role of aqueous processes for the low- and high-NO_x cases. Due to the lack of detailed information about the products resulting from aqueous-phase processes and their volatilities, it is unreasonable to further try to include the aqueous process into the current forward modelling setup. This also means that while the LLEVAP model used in Tikkanen et al. (2020) probably could find a VD solution to reproduce the evaporation curves observed in our study, it would be using incorrect assumptions probably leading to a shift of the modelled VD to higher C* values.

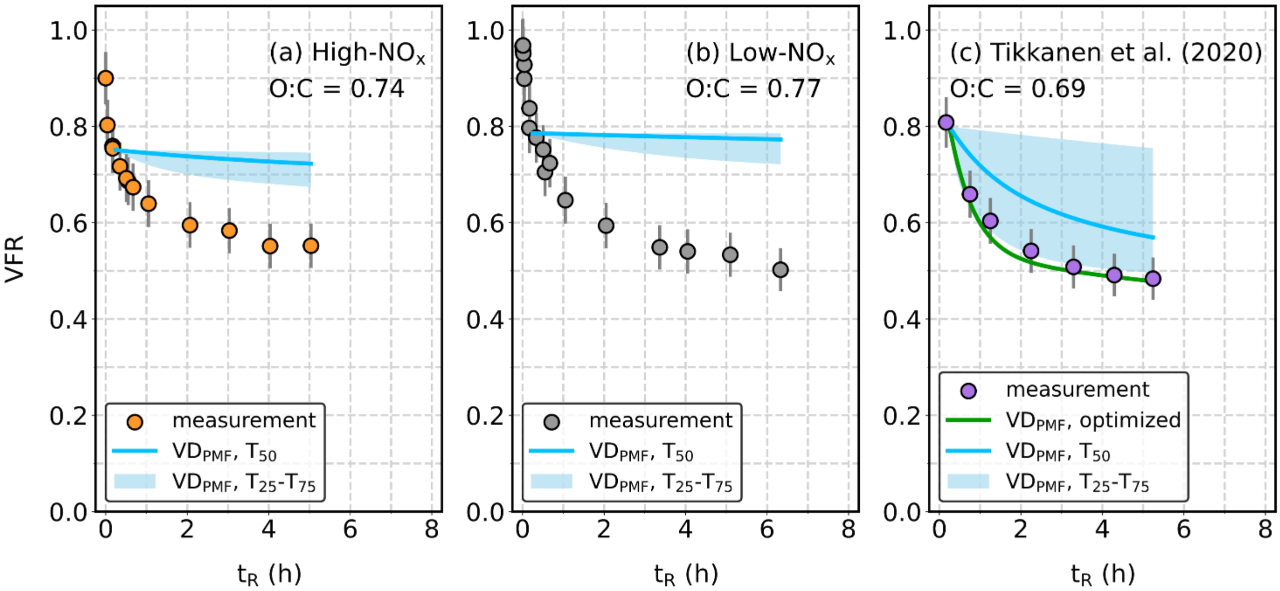

Figure R1. Measured (circles) and simulated (lines and shaded areas) volume fraction remanning (VFR) as function of resisdence time (t_R). The panels (a) and (b) show the data of the high- and low NO$_x$ cases, while the panel (c) displays the data of medium O:C case from Tikkanen et al. (2020). In each panel, the simulations were computed with the T_{50} values (solid blue line) and $T_{25} – T_{75}$ ranges (shaded areas in blue) of the volatility distributions obtained from the FIGAERO-CIMS data (VD$_{PMF}$). The simulation from the optimized VD$_{PMF}$ that was reported by Tikkanen et al. (2020) is shown in solid green line in the panel (c).

b. Further, if modeling the aqueous phase chemistry that occurs at high-RH conditions in the RTC is the main issue here, in my opinion, it is sufficient to restrict the analysis to the RH<7% and/or RH=40% cases.

Response: The extent of aqueous-phase chemistry might be smaller at lower RH due to the decreasing amount of particulate water content, compared to that at high RH. However, the effect of particle viscosity becomes more important with decreasing RH. The process in Tikkanen et al. (2020) was to use the high-RH cases to derive the VD and then use that as an input for the KMGAP model which would find the viscosity for the intermediate- and low-RH cases. Therefore, using only low- and intermediate-RH data would not be enough to derive the VD.

c. In summary, my request would be the following:
   i. add an abbreviated version of Section 2.3 from Tikkanen et al. (2020) to the methods section of this paper
   ii. apply the approach of Tikkanen et al. (2020) to the RH<7% and/or RH=40% high-NOx alpha-pinene SOA evapograms, "fresh" and "RTC" cases that are shown in Fig. 1
   iii. add one figure analogous to Fig 7. from Tikkanen et al. (2020) that compares volatility distributions obtained from evapograms and thermograms of "fresh" and "RTC" high-NOx SOA, and appropriate text to the discussion.

Response: As stated above, we feel that the model-optimization approach used in Tikkanen et al. (2020) is not required here. The presented analysis using forward modelling is enough to answer our research questions. We added a discussion in Section 3.1 in the main text, and also an abbreviated description of the forward modelling in the section S1.1 in SI.

Changes:

Main Text

Section 3.1

[…]

To investigate if particulate water acted also as a catalyzer for aqueous-phase processes for the low- and high-NO_x cases, we calculated the expected isothermal evaporation behavior based on the particle-phase volatility distribution from the PMF analysis of the FIGAERO measurements (see section 3.2) by using a liquid-like evaporation model (LLEVAP) (Lehtinen and Kulmala, 2003; Yli-Juuti et al., 2017), which assumes particle volatility as the only driver for particle size change during particle evaporation (see section S1.1 in Supplement). With this method, Tikkanen et al. (2020) could reproduce the observed isothermal evaporation under high-RH conditions for α-pinene SOA particles if no substantial aqueous-phase processes occurred, and particulate water acted primarily as a plasticizer. But in this study, we found a clear discrepancy between the observed isothermal evaporation and the LLEVAP simulations even when considering the interquartile range of the volatility distribution (see Figure S2 in the Supplement). The volatility distribution derived from the FIGAERO measurement was too far in the LVOC and ELVOC range, i.e., using this volatility distribution always underestimates the amount of isothermal evaporation. This behavior can be interpreted as a sign for aqueous-phase processes. Water acted as a catalyst for reactions creating products of higher volatility which then evaporate from the particle, thus leading to more isothermal evaporation than expected from the original volatility distribution. We discuss more details about the changes in the composition of the residual particles and possible reaction pathways in section 3.4.

[…]

S1.1 Forward modelling for high-RH cases

To model the particle evaporation at high RH, we applied a liquid-like evaporation model (LLEVAP) (Vesala et al., 1997; Lehtinen and Kulmala, 2003; Yli-Juuti et al., 2017). This model assumes there is no concentration gradient existing in the particle. It solves a series of differential equations which describe mass fluxes of organic compounds between particle and gas phase on the basis of gas-phase diffusion, i.e., the difference in the gas-phase concentration of an organic compound near the particle surface and far away for the particle. In this case, the particle-phase volatility distribution (VD) is the only driving factor for the evaporation rate in the model simulation.

Following Tikkanen et al. (2020), we first derived the VD from the positive matrix factorization (PMF) analysis of the FIGAERO measurements (hereafter VD$_{\mathrm{PMF}}$). Afterwards, the derived VD$_{\mathrm{PMF}}$ was used as the initial particle-phase VD in the LLEVAP model. The VD$_{\mathrm{PMF}}$ was derived from the median desorption temperature values (T_{50}), with the interquartile range of desorption temperature ($T_{25} - T_{75}$) in the factor thermograms as the uncertainty. The start time for each LLEVAP simulation was set to the middle time point (i.e., 15 min) of the FIGAERO measurements. In our LLEVAP simulations, we applied the same set of particle properties as Tikkanen et al. (2020). This includes the gas-phase diffusion coefficient, molar mass, particle density, particle surface tension, and mass accommodation coefficient. For each of the two NO$_x$ cases, the LLEVAP simulation is shown in Figure S2a and b. In addition, we included the observation and LLEVPA simulations for α-pinene SOA particle (O : C = 0.69) from Tikkanen et al. (2020), shown in Figure S2c (see also Figure 5a in Tikkanen et al. (2020)). Additionally, Tikkanen et al. (2020) found the best reconstruction of the measured particle evaporation by allowing each PMF factor to vary in the range of $T_{25} - T_{75}$ (VD$_{\mathrm{PMF}}$, optimized, green solid line in Fig S2c).

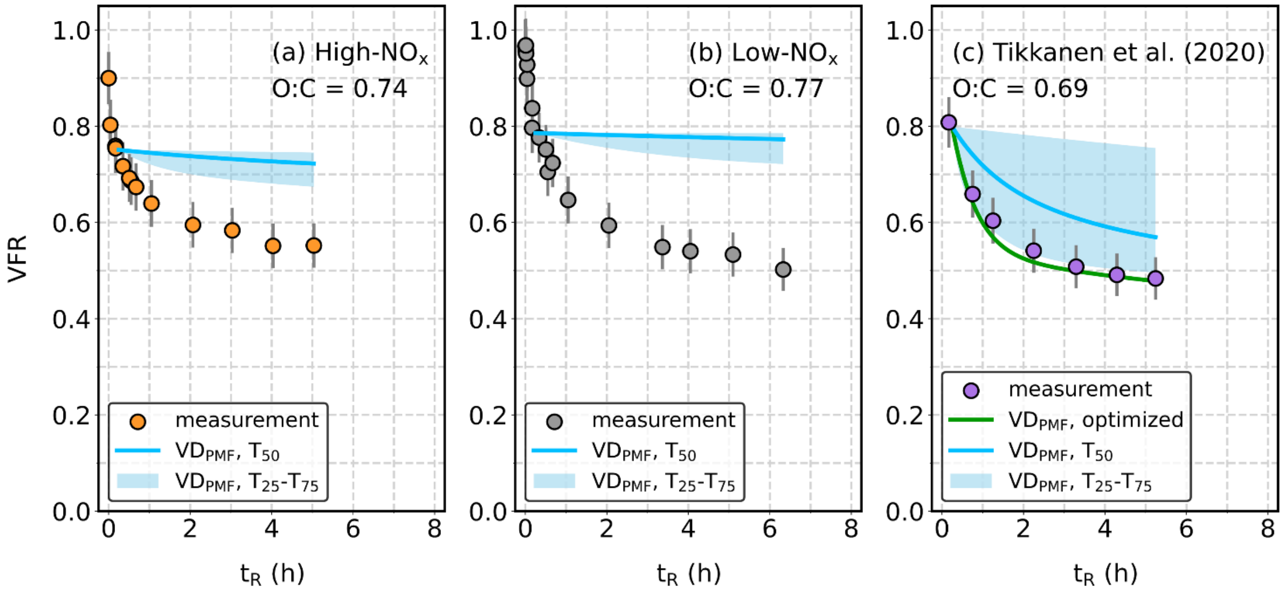

Figure S2. Measured (circles) and LLEVAP-simulated (lines) volume fraction reaming (VFR) as function of residence time (t_R) in the RTC for particles which evaporated under high RH (80% RH) conditions. The panels (a) and (b) show the results of α-pinene SOA particles which were formed under low-NO_x (grey) and high-NO_x (orange) conditions in the OFR, while panel (c) display the result of α-pinene SOA particles (O : C = 0.69) in Tikkanen et al. (2020). In each panel, the simulations were computed with the T_{50} values (solid blue line) and T_{25} – T_{75} ranges (shaded areas in blue) of the volatility distributions obtained from the PMF analysis of the FIGAERO-CIMS data (VD_{PMF}). The simulation from the optimized VD_{PMF} that was reported by Tikkanen et al. (2020) is shown in solid green line in the panel (c).

References

Lehtinen, K. E. J. and Kulmala, M.: A model for particle formation and growth in the atmosphere with molecular resolution in size, Atmos. Chem. Phys., 3, 251-257, DOI 10.5194/acp-3-251-2003, 2003.

Tikkanen, O.-P., Buchholz, A., Ylisirniö, A., Schobesberger, S., Virtanen, A., and Yli-Juuti, T.: Comparing secondary organic aerosol (SOA) volatility distributions derived from isothermal SOA particle evaporation data and FIGAERO–CIMS measurements, Atmos. Chem. Phys., 20, 10441-10458, 2020.

Vesala, T., Kulmala, M., Rudolf, R., Vrtala, A., and Wagner, P. E.: Models for condensational growth and evaporation of binary aerosol particles, J. Aerosol Sci, 28, 565-598, Doi 10.1016/S0021-8502(96)00461-2, 1997.

Yli-Juuti, T., Pajunoja, A., Tikkanen, O. P., Buchholz, A., Faiola, C., Vaisanen, O., Hao, L., Kari, E., Perakyla, O., Garmash, O., Shiraiwa, M., Ehn, M., Lehtinen, K., and Virtanen, A.: Factors controlling the evaporation of secondary organic aerosol from alpha-pinene ozonolysis, Geophys. Res. Lett., 44, 2562-2570, 10.1002/2016GL072364, 2017.